PNAS
www.pnas.org

Supplementary Information for

Heterogeneous and rate-dependent streptavidin-biotin unbinding revealed by high-speed force spectroscopy and atomistic simulations

Felix Rico[1‡*], Andreas Russek[2‡], Laura González[3], Helmut Grubmüller[2*], and Simon Scheuring[4,5*]
[1] Aix Marseille Univ, CNRS, INSERM, LAI, Marseille, France
[2] Department of Theoretical and Computational Biophysics, Am Faßberg 11, Göttingen, Germany
[3] Department of Electronics, Universitat de Barcelona, c/ Marti Franques 1, 08028 Barcelona, Spain
[4] Department of Anesthesiology, Weill Cornell Medical College, 1300 York Ave, New York, NY 10065, USA
[5] Departments of Physiology and Biophysics, Weill Cornell Medical College, 1300 York Ave, New York, NY 10065, USA

[*]Email: felix.rico@inserm.fr, sis2019@med.cornell.edu, hgrubmu@gwdg.de

This PDF file includes:

Supplementary Information Text

Previous single molecule force spectroscopy of the streptavidin/biotin complex. The complex formed by streptavidin (SA) and the small molecule biotin (b, vitamin H) is one of the strongest non-covalent bonds known in nature. Monomeric streptavidin forms the biotin-binding pocket with an eight-stranded, antiparallel beta-barrel capped by loop 3-4. In the native, tetrameric SA, loop 7-8 from an adjacent monomer contributes to closing the binding pocket and was shown important to preserve the binding properties of the complex (60). Biotin binds by forming an intricate network of hydrogen bonds with polar residues of both the beta-barrel and loop 3-4 (4, 5). Due to its high affinity (K_D~10^{-13} M) and long lifetime (k_{off}~10^{-6} s^{-1}, ~0.1 day^{-1}) as measured from bulk, equilibrium measurements (6-9), the SA-b complex is extensively used in molecular biology for protein labeling and purification. SA-b is also widely used in biotechnology and single molecule measurements to immobilize proteins, DNA and RNA molecules on surfaces as it supports large pulling forces (61). The forced disruption of the streptavidin-biotin complex by atomic force microscopy (AFM) and other techniques established the basis of single molecule biomechanics (8-12, 14, 16-21, 28, 62-64). However, single molecule experiments on the SA-b complex often estimated the intrinsic unbinding rate to be orders of magnitude faster than off-rates measured from bulk-equilibrium experiments (~10^{-6} s^{-1}), and data diverge, although this divergence seems to disappear if low binding frequency (highe probability of probing single bonds) is assured (49). Nevertheless, also bulk experiments have reported dissimilar intrinsic unbinding rates (6, 7). All atom steered molecular dynamics simulations (SMDS) of the forced unbinding of SA-b were pioneer in the field and have provided mechanistic descriptions of the unbinding process (26, 27). However, due to limited computational power for SMDS, the number of studies assessing the dynamic nature of the bond are still rare and were performed either on monomeric SA or at pulling velocities several orders of magnitude faster than experiments, precluding direct comparison (26-28, 62, 65-68). Thus, knowledge of the dynamic nature of the SA-b bond and its (un)binding process is still limited, i.e. it is still unknown how this non-covalent bond outlives days.

Bimodal distributions. Bimodal distributions in force histograms have been attributed to simultaneous double bond rupture events and cooperative effects at the high forces reached at fast loading rates (11, 16, 64, 69). Using cantilevers with shorter time response minimized the occurrence of bimodal distributions (**SI**), probably because they allowed easier discrimination between curves with single and double rupture events even at the highest velocities.

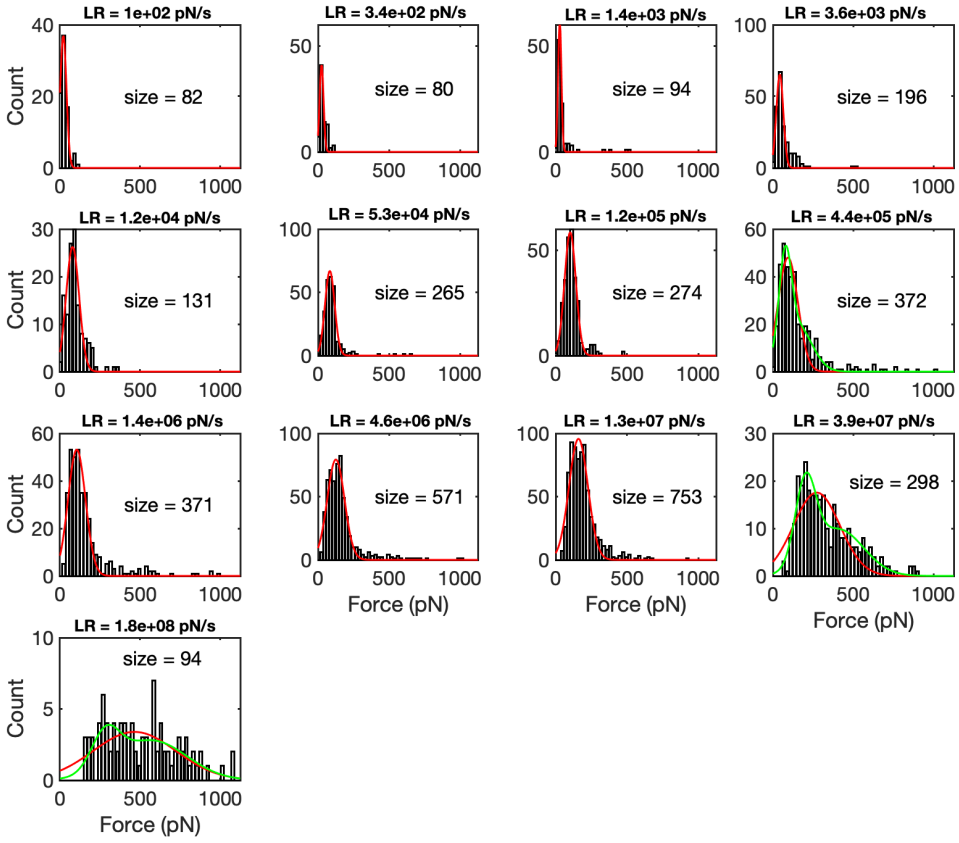

Fig. S1. Rupture force distributions using AC10 cantilevers at different loading rates (LR) indicating the number of analyzed events per plot. Solid lines are best fits to a single (red) and double (green) gaussian distributions. When a double distribution was used, the most probable force was determined from the first peak.

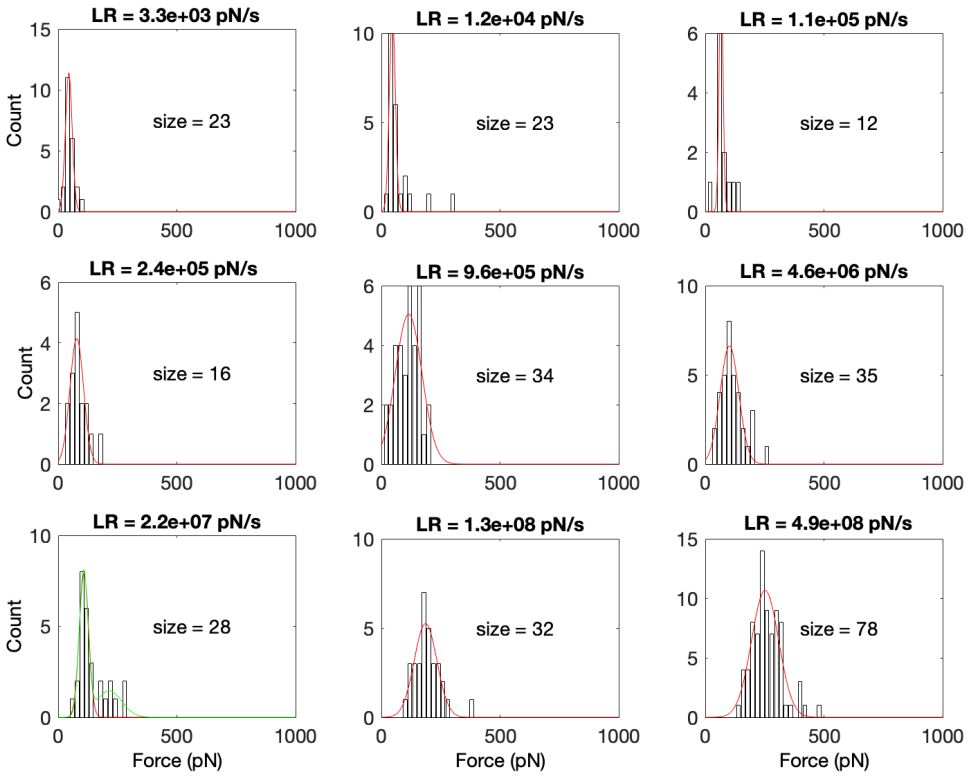

Fig. S2. Rupture force distributions using AC7 cantilevers at different loading rates (LR) indicating the number of analyzed events per plot. Solid lines are best fits to a single (red) and double (green) gaussian distributions. When a double distribution was used, the most probable force was determined from the first peak.

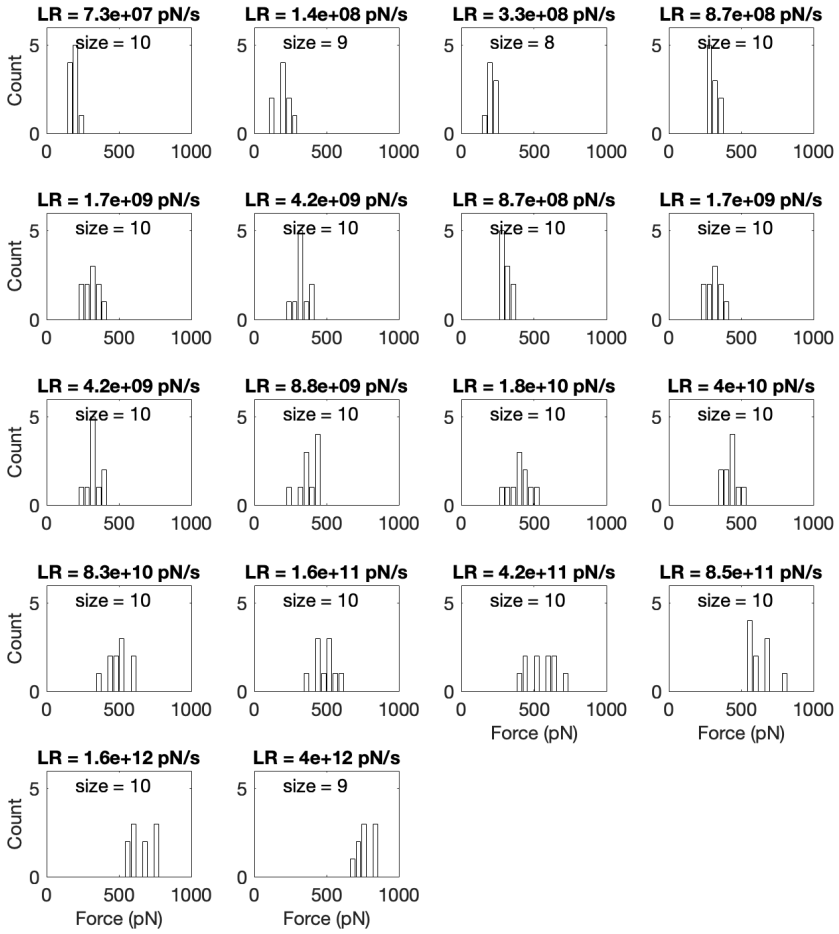

Fig S3. Rupture force distributions from tetrameric SA/b MD simulation trajectories at different loading rates (LR) indicating the number of analyzed events per plot.

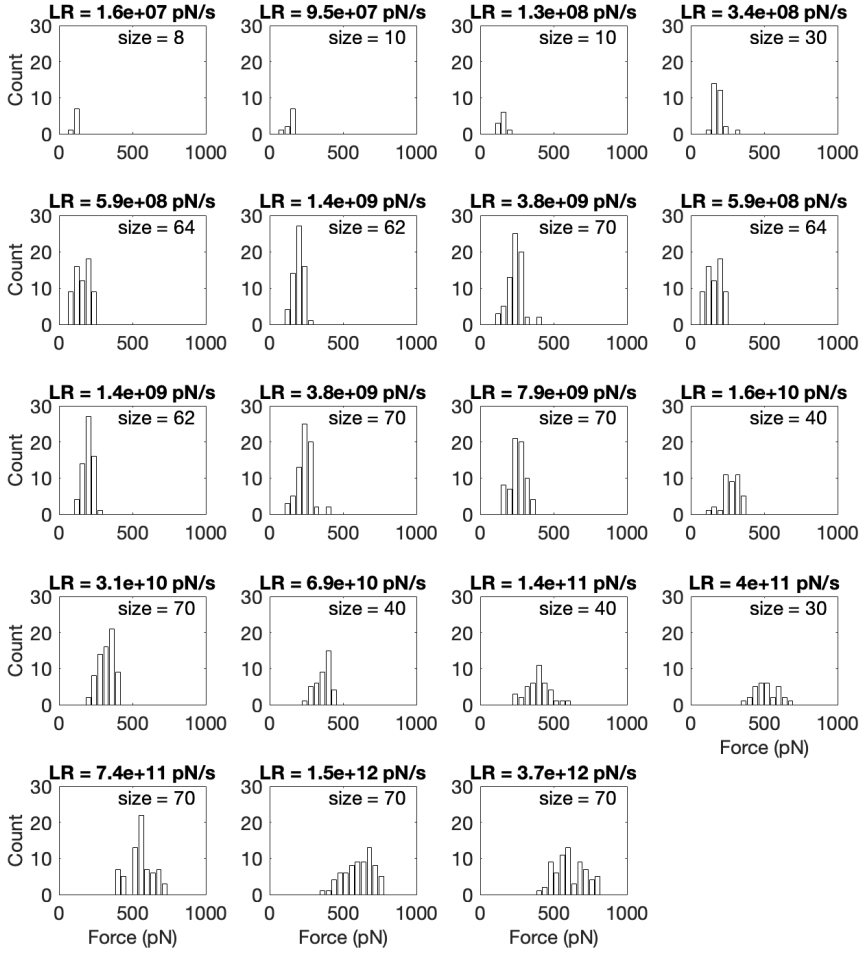

Fig S4. Rupture force distributions from monomeric SA/b MD simulation trajectories at different loading rates (LR) indicating the number of analyzed events per plot.

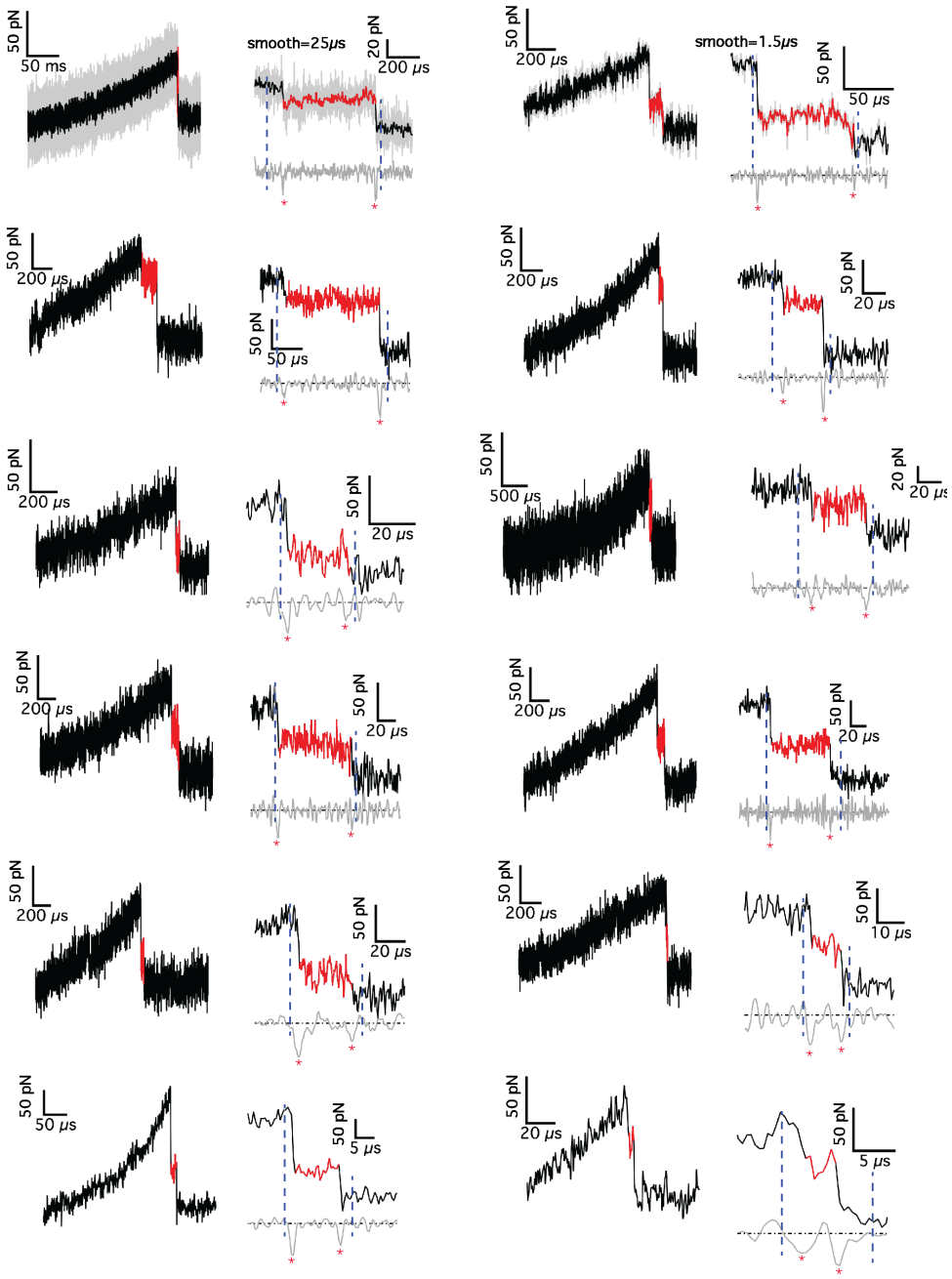

Fig S5. Examples of rupture events (left) showing the zoomed transient binding (right). Raw curves are represented as solid black lines (in grey if smoothed) with transient binding events shown in red. The numerical derivate is shown in grey below the zoomed region (smoothed with a window between 1.5 µs and 25 µs according to pulling velocity and sampling rate). Vertical, dashed blue lines delimit the force drop region analyzed in search of transient binding events. The two most prominent minima within this region are shown with asterisks and were used to determine the lifetime and average force of the transient binding events.

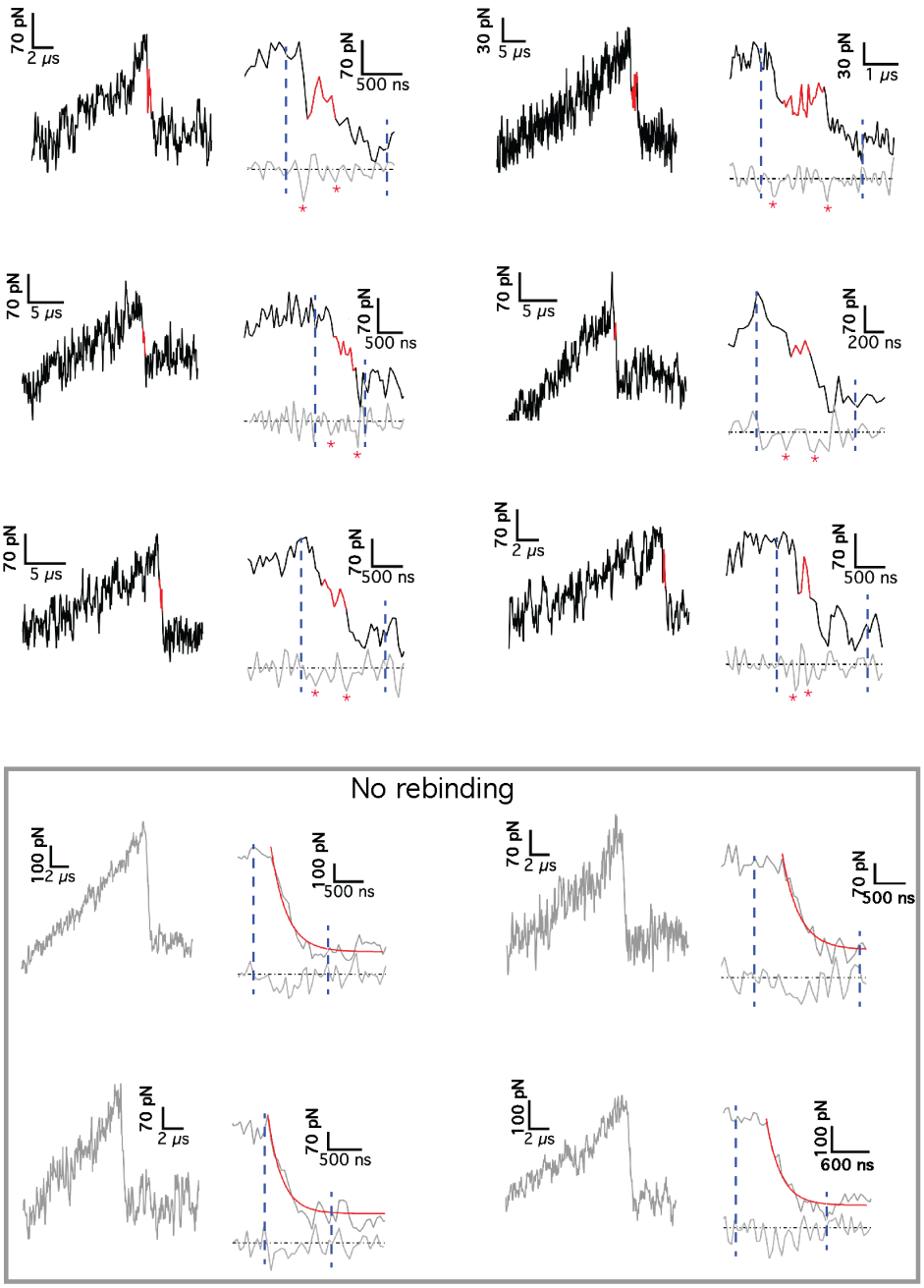

Fig S6. Top six curves: Examples of rupture events (left) showing the zoomed transient binding (right). Raw curves are represented as solid black lines with transient binding events shown in red. The numerical derivate is shown in grey below the zoomed region (no smoothing used. Vertical, dashed blue lines delimit the analyzed region in search of intermediate binding events. The two most prominent minima within this region are shown with asterisks and were used to determine the lifetime and average force of the transient binding event. Four bottom curves: Examples of rupture events without transient binding events (grey solid lines). The red line represents an exponential fit with decay time ranging from 0.22 to 0.32 µs.

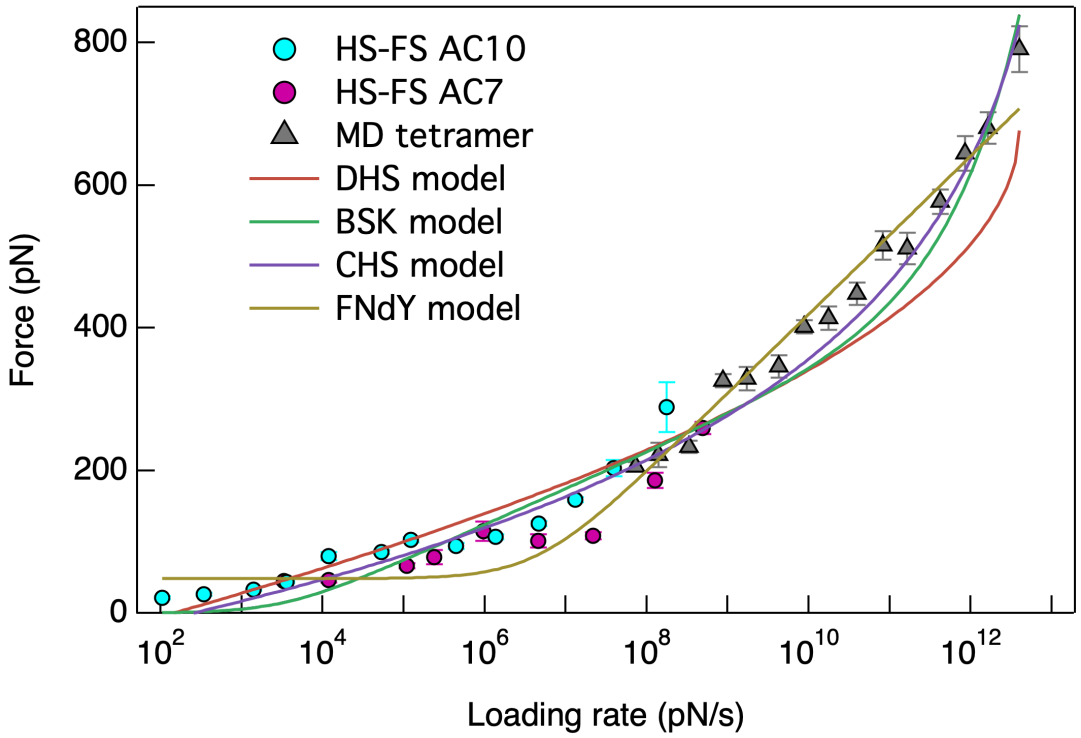

Fig S7. Experimental and MD simulations dynamic force spectra of the SA/b interaction. Solid lines are the best fits of the BSK (15), FNdY (37), DHS (14) and CHS (36) models to the combined dynamic force spectrum. Analytical models were fitted to data using nonlinear least squares weighted with the standard error of the mean. The fitted parameters for each model with error estimations (standard deviation) are reported below. The reported χ^2 is renormalized by the average number of measurements per data point.

DHS
$\chi^2 = 10.4$
$k^0 = 5.7 \pm 2.9$ s^{-1}
$x_\beta = 0.29 \pm 0.02$ nm
$\Delta G = 24.0 \pm 0.1\ k_BT$

BSK
$\chi^2 = 7.7$
$D = (3.9 \pm 1.1)$ x 10^7 nm^2/s
$x_\beta = 0.18 \pm 0.01$ nm
$\Delta G = 20.4 \pm 0.1\ k_BT$

FNdY
$\chi^2 = 10.6$
$F_{eq} = 48 \pm 6$ pN
$x_\beta = 0.08 \pm 0.01$ nm
$k^0 = 19646 \pm 8490$ s^{-1}

CHS
$\chi^2 = 4.9$
$k^0 = 0.02 \pm 0.01$ s^{-1}
$x_\beta = 0.34 \pm 0.03$ nm
$\Delta G = 25.0 \pm 0.1\ k_BT$
$\mu = (2.7 \pm 17)$ x 10^{-5}

BD
$\chi^2 = 4.8$
$\Delta G_1 = 16.9 \pm 0.2\ k_BT$
$\Delta G_2 = 20.7 \pm 0.7\ k_BT$
$x_{\beta 1} = 0.19 \pm 0.02$ nm
$x_{\beta 2} = 0.44 \pm 0.07$ nm
$\omega_1 = 0.9 \pm 0.4$
$\omega_2 = 1.7 \pm 0.7$
$D = 4.0$ x 10^7 nm^2/s

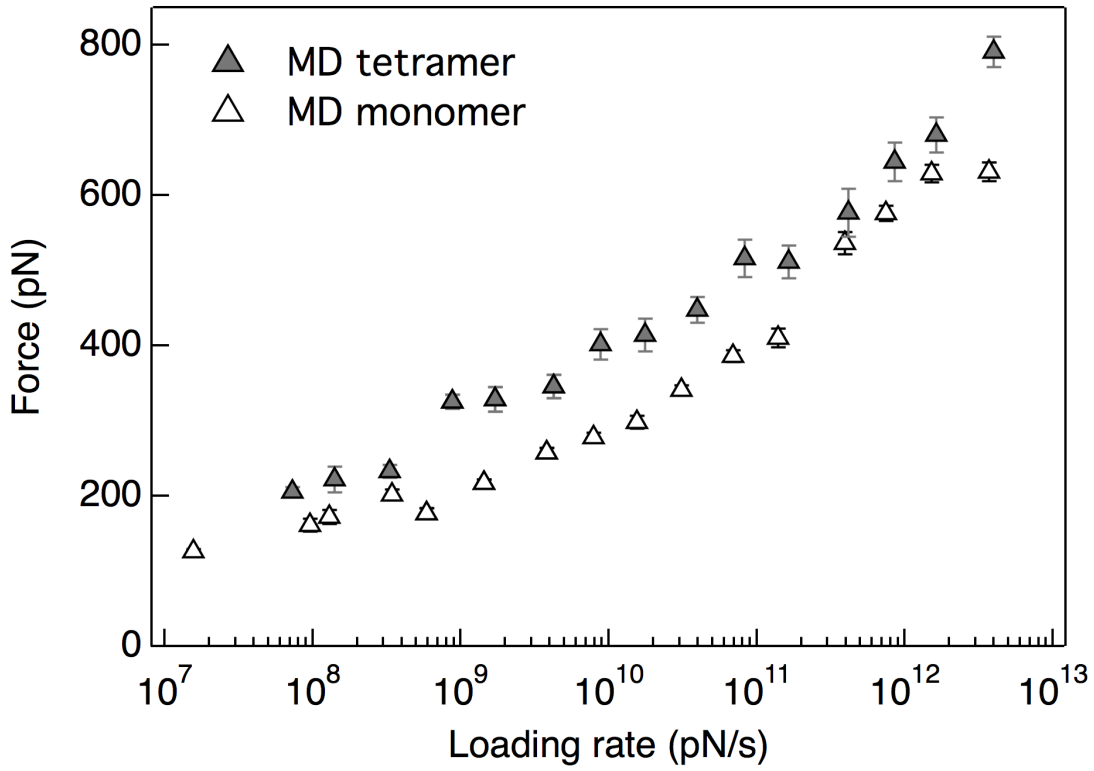

Fig. S8. Comparison between monomeric and tetrameric streptavidin-biotin MD force spectra.

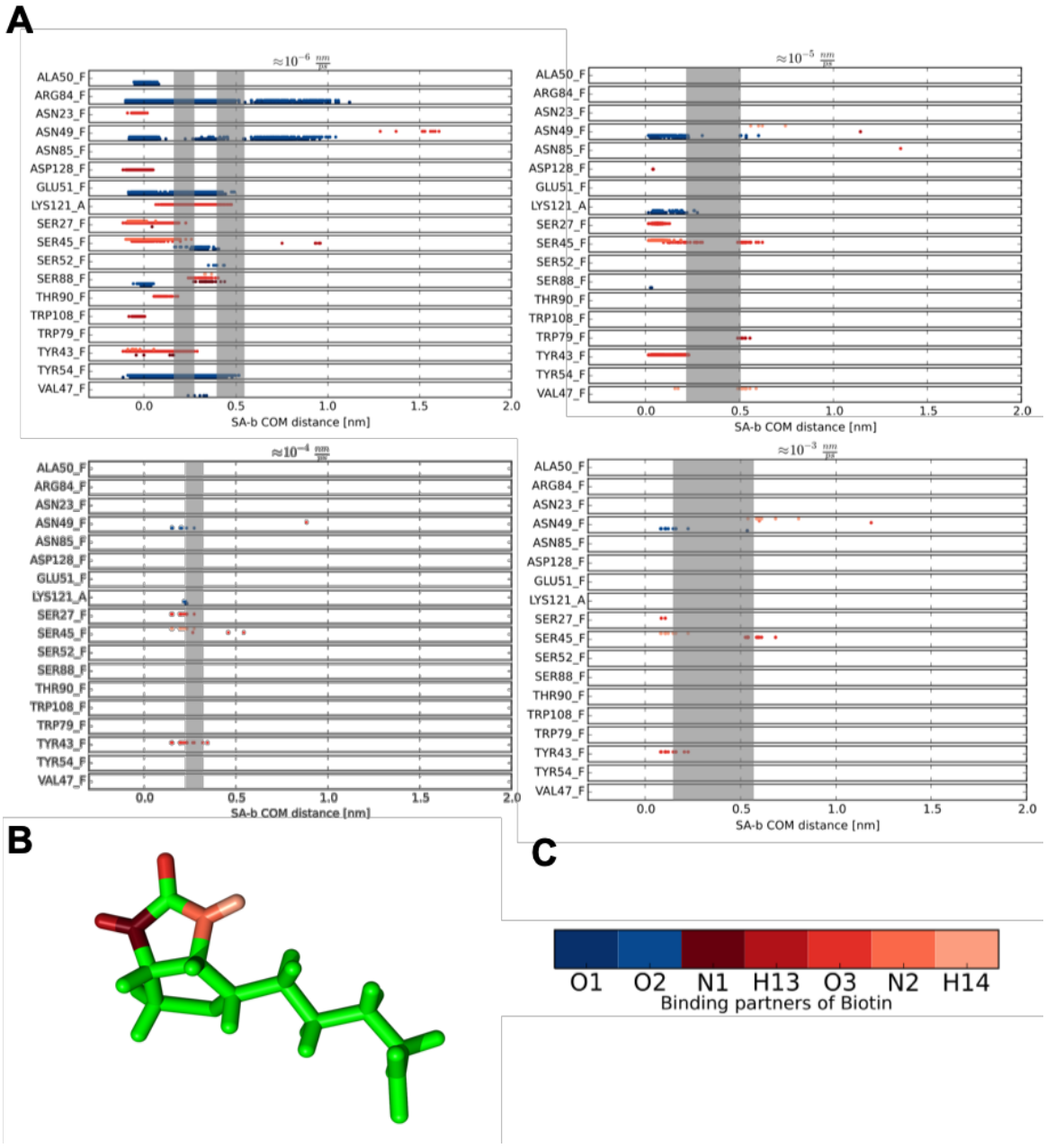

Fig. S9. Examples of simultaneous bond rupture of H-bonds with subsequent building of new binding patterns (grey background) at the 4 different velocity regimes named in the titles. For easier comparison, each subplot shows all interacting amino acids, even if no H-bond was formed. The existence of H-bonds between the named amino acids and biotin is shown as colored dots. F stands for the SA monomer out of which biotin is pulled and A (see Lys121) for an adjacent SA monomer. The color of the dots refers to the interaction partner of biotin shown in B as stick representation. Red colors stand for interactions with the head group of biotin as shown in B. The blue dots are H-bonds formed with the tail of biotin. C Color bar showing the used color-code in A.

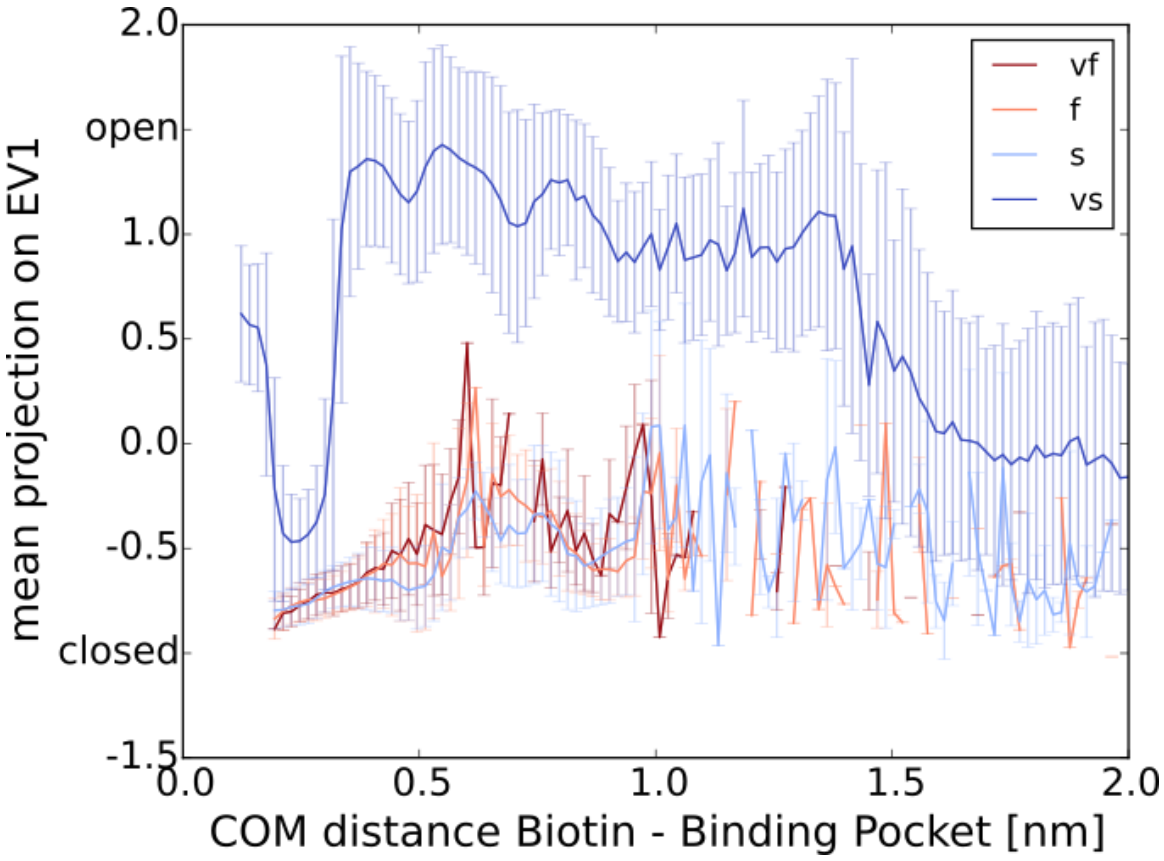

Fig. S10. Projection of all trajectories onto the first eigenvector of a PCA of the loop3-4 motion plotted over the COM distance between the binding pocket and biotin. Different colors denote different pulling velocity regimes ranging from very fast (vr, red) to very slow (vs, blue).

Movies

Video S1. Representative movie of an unbinding trajectory from MD simulations of tetrameric SA/b at 1 m/s pulling velocity.

Video S2. Representative movie of an unbinding trajectory from MD simulations of tetrameric SA/b at 0.2 m/s pulling velocity.

Video S3. Representative movie of an unbinding trajectory from MD simulations of tetrameric SA/b at 0.01 m/s pulling velocity.

Video S4. Representative movie of an unbinding trajectory from MD simulations of monomeric SA/b at 1 m/s pulling velocity.

Video S5. Representative movie of an unbinding trajectory from MD simulations of monomeric SA/b at 0.1 m/s pulling velocity.

Video S6. Representative movie of an unbinding trajectory from MD simulations of monomeric SA/b at 0.01 m/s pulling velocity.

References

60. Freitag S, Le Trong I, Klumb L, Stayton P, & Stenkamp R (1997) Structural studies of the streptavidin binding loop. *Protein science: a publication of the Protein Society* 6(6):1157-1166.
61. Neuman KC, Lionnet T, & Allemand JF (2007) Single-Molecule Micromanipulation Techniques. *Annual Review of Materials Research* 37(1):33-67.
62. Zhou J*, et al.* (2006) Unbinding of the streptavidin-biotin complex by atomic force microscopy: A hybrid simulation study. *J. Chem. Phys.* 125(10):104905.
63. Pierres A, Touchard D, Benoliel AM, & Bongrand P (2002) Dissecting streptavidin-biotin interaction with a Laminar flow chamber. *Biophysical Journal* 82(6):3214-3223.
64. Guo S, Ray C, Kirkpatrick A, Lad N, & Akhremitchev BB (2008) Effects of Multiple-Bond Ruptures on Kinetic Parameters Extracted from Force Spectroscopy Measurements: Revisiting Biotin-Streptavidin Interactions. *Biophysical Journal* 95(8):3964-3976.
65. Hyre DE*, et al.* (2002) Early mechanistic events in biotin dissociation from streptavidin. *Nat. Struct. Biol.* 9(8):582-585.
66. Freitag S*, et al.* (1999) A structural snapshot of an intermediate on the streptavidin-biotin dissociation pathway. *Proc. Natl. Acad. Sci. U. S. A.* 96(15):8384-8389.
67. Milles LF, Schulten K, Gaub HE, & Bernardi RC (2018) Molecular mechanism of extreme mechanostability in a pathogen adhesin. *Science* 359(6383):1527-1533.
68. O'Sullivan VJ*, et al.* (2012) Development of a Tetrameric Streptavidin Mutein with Reversible Biotin Binding Capability: Engineering a Mobile Loop as an Exit Door for Biotin. *PLoS ONE* 7(4):e35203.
69. Zhang XH & Moy VT (2003) Cooperative adhesion of ligand-receptor bonds. *Biophys. Chem.* 104(1):271-278.